UCSF

Title
The genetic landscape of gliomas arising after therapeutic radiation

Permalink

Journal

ISSN

Authors
López, Giselle Y
Van Ziffle, Jessica
Onodera, Courtney
et al.

Publication Date

DOI

Peer reviewed

ORIGINAL ARTICLE

The genetic landscape of gliomas arising after therapeutic radiation

Giselle Y. López[1,2] · Jessica Van Ziffle[1,3] · Courtney Onodera[1,3] · James P. Grenert[1,3] · Iwei Yeh[1,3,4] · Boris C. Bastian[1,3,4] · Jennifer Clarke[5,6] · Nancy Ann Oberheim Bush[5,6] · Jennie Taylor[5,6] · Susan Chang[5] · Nicholas Butowski[5] · Anuradha Banerjee[7] · Sabine Mueller[6,7] · Cassie Kline[6,7] · Joseph Torkildson[8] · David Samuel[9] · Aleli Siongco[10] · Corey Raffel[2] · Nalin Gupta[2,11] · Sandeep Kunwar[2] · Praveen Mummaneni[2] · Manish Aghi[2] · Philip Theodosopoulos[2] · Mitchel Berger[2] · Joanna J. Phillips[1,2] · Melike Pekmezci[1] · Tarik Tihan[1] · Andrew W. Bollen[1] · Arie Perry[1,2] · David A. Solomon[1,3]

Abstract

Radiotherapy improves survival for common childhood cancers such as medulloblastoma, leukemia, and germ cell tumors. Unfortunately, long-term survivors suffer sequelae that can include secondary neoplasia. Gliomas are common secondary neoplasms after cranial or craniospinal radiation, most often manifesting as high-grade astrocytomas with poor clinical outcomes. Here, we performed genetic profiling on a cohort of 12 gliomas arising after therapeutic radiation to determine their molecular pathogenesis and assess for differences in genomic signature compared to their spontaneous counterparts. We identified a high frequency of *TP53* mutations, *CDK4* amplification or *CDKN2A* homozygous deletion, and amplifications or rearrangements involving receptor tyrosine kinase and Ras–Raf–MAP kinase pathway genes including *PDGFRA*, *MET*, *BRAF*, and *RRAS2*. Notably, all tumors lacked alterations in *IDH1*, *IDH2*, *H3F3A*, *HIST1H3B*, *HIST1H3C*, *TERT* (including promoter region), and *PTEN*, which genetically define the major subtypes of diffuse gliomas in children and adults. All gliomas in this cohort had very low somatic mutation burden (less than three somatic single nucleotide variants or small indels per Mb). The ten high-grade gliomas demonstrated markedly aneuploid genomes, with significantly increased quantity of intrachromosomal copy number breakpoints and focal amplifications/homozygous deletions compared to spontaneous high-grade gliomas, likely as a result of DNA double-strand breaks induced by gamma radiation. Together, these findings demonstrate a distinct molecular pathogenesis of secondary gliomas arising after radiation therapy and identify a genomic signature that may aid in differentiating these tumors from their spontaneous counterparts.

Keywords Secondary malignancy · Radiation therapy · Ionizing radiation · Radiation-associated glioma · Radiation-induced glioma (RIG) · DNA double-strand breaks · Chromosome breaks · Genomic signature · Mutational signature · Glioblastoma · Astrocytoma · Ganglioglioma

Introduction

Ionizing radiation has been used for cancer therapy for more than 100 years, dating back to Drs. Emil Grubbe and Victor Despeignes who are credited with the first use of medical radiation in the late 1800s [15]. Radiation therapy (XRT)

has proven benefit in helping to cure or extend survival for cancer patients, particularly for some of the more radiosensitive tumor types such as lymphoma and germ cell tumors. However, XRT is accompanied by side effects, both acute and late. Late side effects include lymphedema resulting from damage to the lymphatic system, neuropathy resulting from damage to peripheral nerves, vasculopathies resulting from damage to endothelial cells, cognitive impairment, and many others. One of the most serious late consequences of XRT is secondary neoplasia, which occurs in only a minority of patients but represents a major cause of mortality in long-term survivors of childhood malignancies. Within the brain, the most common secondary neoplasms arising after

✉ David A. Solomon
  david.solomon@ucsf.edu

Extended author information available on the last page of the article

radiation therapy are meningiomas, gliomas, and sarcomas [11, 31]. Such radiation-induced gliomas are typically high-grade infiltrative astrocytomas associated with poor outcomes [11, 29, 31, 33].

Over the past two decades, the genetic alterations responsible for each of the major subtypes of spontaneous gliomas have been identified. For example, we now know that primary glioblastomas arising in the cerebral hemispheres of older adults are genetically defined by frequent *TERT* promoter mutation, *CDKN2A* homozygous deletion, *EGFR* amplification plus mutation/rearrangement, trisomy 7, monosomy 10, and *PTEN* mutation or deletion [8, 9]. Diffuse lower-grade gliomas in the cerebral hemispheres of younger adults are genetically defined by a recurrent hotspot mutation in either the *IDH1* or *IDH2* oncogenes, with additional *TERT* promoter mutation and chromosomes 1p and 19q co-deletion in oligodendroglial neoplasms versus additional *ATRX* and *TP53* mutations in diffuse astrocytic neoplasms [10, 13]. In children, diffuse gliomas arising in midline structures of the CNS are defined by p.K27M mutation in the *H3F3A*, *HIST1H3B*, or *HIST1H3C* genes, which are accompanied by a spectrum of additional alterations frequently involving *TP53*, *PPM1D*, *ACVR1*, *PDGFRA*, and *PIK3CA* [19, 30, 32]. In contrast, diffuse gliomas arising in the cerebral hemispheres of children are often defined by mutually exclusive *H3F3A* p.G34R/V or *SETD2* mutations, which are accompanied by frequent *TP53*, *ATRX*, and *PDGFRA* alterations [14, 19, 21, 32]. However, the genetic alterations that are responsible for secondary gliomas arising after radiation therapy are largely unknown, with some studies suggesting differences with their spontaneous counterparts based on either gene expression analysis or single gene testing for *IDH1/2* mutation or *EGFR* amplification [5, 12, 16, 20, 21, 24].

Studying the mutational and chromosomal patterns in thousands of human cancers across the spectrum of different cancer types has identified "mutational signatures" that are associated with specific cancer types and with specific mutational processes, including the intrinsic infidelity of the DNA replication machinery, exogenous or endogenous mutagen exposures, enzymatic modification of DNA, and defective DNA repair [2]. For example, Mutational Signature 6 caused by mismatch repair deficiency is characterized by a predominance of small indels and C>T transitions and is seen most commonly in endometrial and colorectal carcinomas. In contrast, Mutational Signature 7 caused by ultraviolet irradiation is characterized by a predominance of C>T mononucleotide and CC>TT dinucleotide transitions and is seen most commonly in cutaneous melanomas and squamous cell carcinomas arising on sun-exposed skin. One recent study assessed the mutational signature in a small cohort of radiation-associated osteosarcomas, spindle cell sarcomas, angiosarcomas, and breast cancers, which

identified an excess of balanced inversions and small deletions (1–100 base pairs in size with microhomology at the junctions) compared to a cohort of spontaneous tumors [3]. These results suggest that the DNA double-strand breaks induced by ionizing radiation generate a distinct scar in the genome that may cause the activation of oncogenes and inactivation of tumor suppressor genes responsible for secondary malignancies. Two recent studies of radiation-induced meningiomas found that they lacked somatic single nucleotide variants in the most common genes associated with spontaneous meningioma development including *NF2*, *TRAF7*, *AKT1*, *SMO*, and *KLF4*. Instead, they harbored frequent structural rearrangements involving the *NF2* tumor suppressor gene, which are only rarely seen in spontaneous meningiomas [1, 28]. Together, these studies provide preliminary evidence that the DNA double-strand breaks caused by ionizing radiation may lead to a distinct genomic signature and gene alterations that drive radiation-induced secondary malignancies.

Herein, we performed comprehensive molecular profiling on a cohort of 12 secondary gliomas arising after radiation therapy to evaluate the responsible genetic alterations and to assess for a genomic signature that may aid in differentiating these tumors from their spontaneous counterparts.

Methods

Patients and tumor tissue

We searched our institutional pathology archives for cases of radiation-associated glioma that met the following four criteria: (1) treatment with radiation for a prior non-glial neoplasm, (2) interval between initial radiation therapy and development of secondary glioma of greater than 2 years, (3) development of the glioma within the radiation field, and (4) no known family history of tumor predisposition syndrome. Twelve patients were identified meeting these criteria with available diagnostic slides and tissue blocks containing sufficient tumor tissue for genetic analysis. All tumor specimens, spanning years 2008–2017, had been fixed in 10% neutral-buffered formalin and embedded in paraffin. Clinical data were extracted from institutional electronic medical records including patient sex, age at diagnosis of primary non-glial malignancy, pathologic type and anatomic site of primary malignancy, radiation treatment field and dose, time interval between radiation therapy and development of secondary glioma, histologic subtype and anatomic site of secondary glioma, therapy received for radiation-associated glioma, and clinical outcome.

To assess for differences in genomic signature of the radiation-associated gliomas compared to their spontaneous counterparts, we compared the sequencing results from

the radiation-associated gliomas to a cohort of 12 spontaneous IDH-wildtype glioblastomas in the cerebral hemispheres of adults, 12 spontaneous IDH-mutant glioblastomas in the cerebral hemispheres of adults, 12 spontaneous H3 K27M-mutant diffuse midline gliomas in children, and 12 spontaneous IDH- and H3 K27-wildtype high-grade infiltrative gliomas in children. These spontaneous gliomas were all treatment naïve and consisted of the 12 most recent tumors belonging to each of these four different entities that were sequenced on a clinical basis at UCSF Medical Center.

Genomic DNA extraction and targeted next-generation sequencing

Genomic DNA was extracted from tumor tissue that had been macrodissected from formalin-fixed, paraffin-embedded blocks or unstained sections using the QIAamp DNA FFPE Tissue Kit (Qiagen) according to the manufacturer's protocol. For 6 of the 12 patients (#3, 6, 7, 8, 9, and 12), genomic DNA was also extracted from a peripheral blood sample using the QIAamp DNA Blood Midi Kit (Qiagen). Capture-based next-generation DNA sequencing was performed as previously described at the UCSF Clinical Cancer Genomics Laboratory [17, 18, 22, 23], using an assay that targets all coding exons of 479 cancer-related genes, *TERT* promoter, select introns, and upstream regulatory regions of 47 genes to enable detection of structural variants including gene fusions, and DNA segments at regular intervals along each chromosome to enable genome-wide copy number and zygosity analysis, with a total sequencing footprint of 2.8 Mb [UCSF500 Cancer Panel; Supplementary Table 1 (Online Resource 1)]. Sequencing libraries were prepared from genomic DNA, and target enrichment was performed by hybrid capture using a custom oligonucleotide library (Roche NimbleGen). Sequencing was performed on an Illumina HiSeq 2500. Duplicate sequencing reads were removed computationally to allow for accurate allele frequency determination and copy number calling. The analysis was based on the human reference sequence (NCBI build 37) using the following software packages: BWA, Samtools, Picard tools, GATK, CNVkit, Pindel, SATK, Annovar, Freebayes, and Delly. Single nucleotide variants, insertions/deletions, and structural variants were visualized and verified using the Integrated Genome Viewer. Genome-wide copy number analysis and assessment of intrachromosomal copy number breakpoints were performed using CNVkit and Nexus Copy Number (Biodiscovery).

Statistical analysis

Statistical analysis was performed using GraphPad Prism software version 7. Comparison of the quantity of intrachromosomal copy number breakpoints per genome, quantity of chromosomes with ≥ 4 intrachromosomal copy number breakpoints, and quantity of focal amplifications or homozygous deletions between radiation-associated high-grade gliomas and spontaneous high-grade gliomas was performed using Mann–Whitney unpaired two-tailed t test.

Data availability

Sequencing data files are available from the authors upon request.

Results

Clinicopathologic features of patients with radiation-associated gliomas

Twelve patients with secondary gliomas arising after radiation treatment for a primary non-glial neoplasm were included in this study [Table 1 and Supplementary Table 2 (Online Resource 1)]. None of the patients were known to have a familial tumor predisposition syndrome. The eight males and four females ranged in age at the time of diagnosis of the primary neoplasm from 1 to 32 years (median 14 years). Primary neoplasms were medulloblastoma ($n=5$), intracranial germinoma (2), leukemia (2), Hodgkin's lymphoma (1), craniopharyngioma (1), and pineocytoma (1). Radiation treatment was variable; examples include 18 Gy of craniospinal radiation at CNS relapse for acute lymphoblastic leukemia, 55 Gy of cranial radiation for craniopharyngioma, and 36 Gy of craniospinal radiation with 19 Gy boost to the posterior fossa for medulloblastoma. The interval between radiation therapy and secondary glioma diagnosis ranged from 4 to 41 years (mean 16 years). Patient #11 with the longest interval (41 years) had undergone resection of multiple meningiomas, presumably radiation induced, following craniospinal radiation during infancy for leukemia before the glioma diagnosis. Ten of the secondary gliomas were high-grade infiltrative astrocytomas, either anaplastic astrocytoma or glioblastoma [histology from representative cases is shown in Supplementary Fig. 1 (Online Resource 2)]. The secondary glioma in patient #11 was an exophytic lesion arising from the posterior medulla for which a histologic diagnosis of pleomorphic xanthoastrocytoma, WHO grade II, had been made [Supplementary Fig. 1 (Online Resource 2)]. The secondary glioma in patient #12 was a solid and cystic lesion in the left frontal lobe of the brain for which a histologic diagnosis of ganglioglioma, WHO grade I, had been made [Supplementary Fig. 1 (Online Resource 2)]. Among the seven patients with secondary high-grade gliomas with available follow-up data, five had survived less than 2 years after diagnosis, and the other two had progressive disease but were still alive during a limited follow-up

Table 1 Clinical and pathologic features of the 12 patients with gliomas arising after radiation therapy

Patient #	Primary neoplasm	Site of primary neoplasm	Age at initial dx (years)	XRT-associated glioma histologic diagnosis	Site of XRT-associated glioma	Interval between radiation therapy and glioma dx (years)
1	Craniopharyngioma	Sellar	14	Glioblastoma	Left temporal lobe	27
2	Germinoma	Sellar and pineal	21	Glioblastoma	Right cerebellum	23
3	Medulloblastoma	Cerebellum/fourth ventricle	7	Glioblastoma	Right cerebellum	13
4	Pineocytoma	Pineal	31	Glioblastoma	Right thalamus and midbrain	4
5	Medulloblastoma	Cerebellum/fourth ventricle	32	Glioblastoma	Cerebellum/fourth ventricle	5
6	Medulloblastoma	Cerebellum/fourth ventricle	5	Anaplastic astrocytoma	Brainstem with CSF dissemination	10
7	Acute lymphoblastic leukemia	Systemic with CNS relapse	2	Anaplastic astrocytoma	Right frontal lobe	5
8	Medulloblastoma	Cerebellum/fourth ventricle	5	Glioblastoma	Pons	10
9	Germinoma	Sellar	32	Anaplastic astrocytoma	Brainstem with diffuse gliomatosis	16
10	Hodgkin's lymphoma	Thoracic lymph nodes	26	Glioblastoma	Thoracic spinal cord	21
11	Leukemia	Systemic	1	Pleomorphic xanthoastrocytoma	Medulla/fourth ventricle	41
12	Medulloblastoma	Cerebellum/fourth ventricle	6	Ganglioglioma	Left frontal lobe	19

period of less than 1 year. Patient #12 with a secondary ganglioglioma was alive with no evidence of recurrence at 13 months after resection.

Genetic features of radiation-associated gliomas

Targeted next-generation sequencing that provides assessment of mutations, gene fusions, amplifications, deletions, and chromosomal copy number alterations was performed on the cohort of 12 radiation-associated gliomas [Fig. 1 and Supplementary Tables 3–6 (Online Resource 1)].

Among the ten high-grade gliomas, seven cases harbored inactivating mutations in the *TP53* tumor suppressor gene with loss of the remaining wildtype allele (70%). Four cases harbored focal homozygous deletions of the *CDKN2A* and *CDKN2B* tumor suppressor genes (40%), while four other cases harbored focal high-level amplifications of the *CDK4* oncogene (40%), one of which additionally harbored focal high-level amplification of *CCND3*. In total, 8/10 of the high-grade gliomas had genetic alterations disrupting cell cycle regulation (80%). Focal high-level amplifications or pathogenic mutations involving receptor tyrosine kinase genes were seen in eight cases (80%), with five cases harboring *PDGFRA* amplification, two cases harboring *MET* amplification, and one case harboring *EGFR* amplification. Two of the cases with *PDGFRA* amplification harbored missense mutations on the amplified allele located

in the extracellular ligand-binding domain (p.Y249C and p.G286R), and one of the cases with *MET* amplification harbored a missense mutation on the amplified allele located in the extracellular ligand-binding domain (p.A179T). One case (#8) lacking amplification of receptor tyrosine kinase genes harbored three missense mutations in *PDGFRA*, all of which were located in the intracellular portion of the protein (p.P577R, p.P653L, and p.H845D), of which the p.H845D variant affected a codon within the tyrosine kinase domain that is recurrently mutated in gliomas and gastrointestinal stromal tumors (Catalog of Somatic Mutations In Cancer database, version 85 release). Four of the cases harbored alterations in components of the Ras–Raf–MAP kinase signaling pathway (40%), including both cases (#6 and 7) lacking alterations in receptor tyrosine kinase genes. Two cases harbored focal high-level amplifications of *RRAS2*, one of which also harbored a nonsense mutation in *NF1*, and two other cases harbored rearrangements of *BRAF*, one with intragenic deletion of exon 4 and one with *GTF2I–BRAF* gene fusion. Three cases harbored pathogenic alterations in components of the PI3-kinase–Akt–mTOR signaling pathway (30%). One case harbored an activating hotspot mutation in *PIK3CA* (p.Q546R), one case harbored focal high-level amplification of *AKT3*, and one case harbored a truncating frameshift mutation in *TSC2*. Focal high-level amplifications of *MYCN* and *MYCL1* were each present in one case. Alterations in other transcriptional regulatory
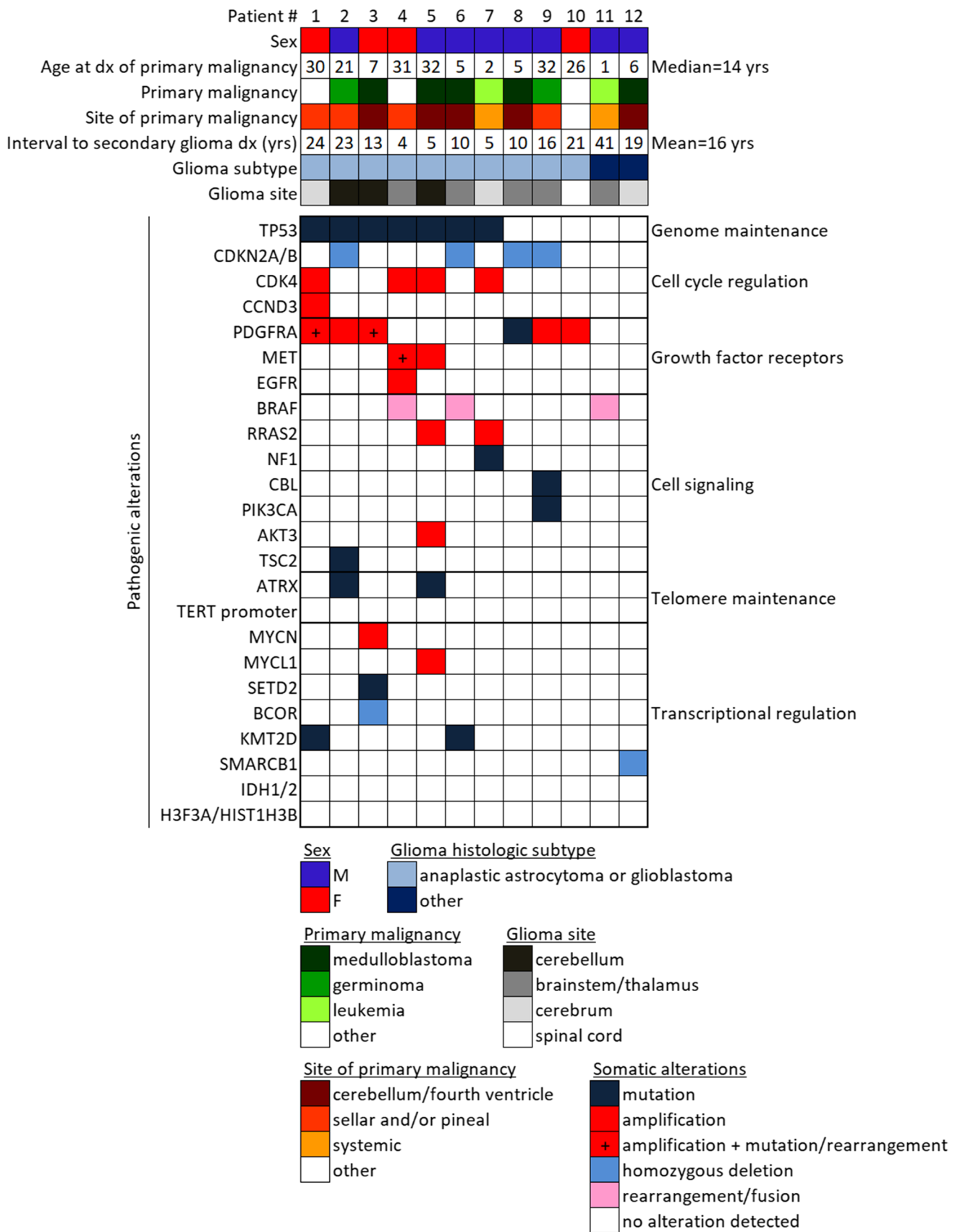
Fig. 1 Oncoprint summary table of the 12 patients with secondary gliomas arising after radiation therapy

genes were present in three cases, including two with *KMT2D* mutations and one with both *BCOR* focal homozygous deletion and a frameshift mutation in *SETD2*. Two cases harbored truncating mutations in *ATRX*, which has been associated with alternative lengthening of telomeres. However, the remaining eight high-grade gliomas all lacked *TERT* amplification, promoter hotspot mutation, or rearrangement. None of the cases harbored pathogenic mutations, amplifications, deletions, and rearrangements in *IDH1*, *IDH2*, *H3F3A*, *HIST1H3B*, *HIST1H3C*, *PPM1D*, *ACVR1*, *FGFR1*, *FGFR2*, *FGFR3*, *NTRK1*, *NTRK2*, *NTRK3*, and *PTEN*.

The secondary glioma arising from the posterior medulla in patient #11 with histologic features of pleomorphic xanthoastrocytoma was found to harbor *KIAA1549–BRAF* gene fusion as the solitary pathogenic alteration. No *CDKN2A* deletion or mutation characteristic of pleomorphic xanthoastrocytoma was identified [25, 26]. The secondary glioma in the left frontal lobe of patient #12 with histologic features of ganglioglioma was found to harbor focal homozygous deletion of the *SMARCB1* gene as the solitary pathogenic alteration, and immunohistochemical staining demonstrated somatic loss of the encoded SMARCB1/BAF47/INI-1 chromatin remodeling protein in the tumor cells [Supplementary Fig. 1 (Online Resource 2)]. No *BRAF* mutation or other alteration in the Ras–Raf–MAP kinase pathway characteristic of ganglioglioma was identified [23].

For patient #3, genetic profiling was performed on both the medulloblastoma with classic histology resected from the fourth ventricle at 7 years of age and the glioblastoma resected from the right cerebellum at 19 years of age [Fig. 2 and Supplementary Fig. 2 (Online Resource 2)]. The medulloblastoma demonstrated a hotspot missense mutation in the *CTNNB1* oncogene (p.G34V), a frameshift mutation in the *ARID2* chromatin remodeling gene, monosomy 6, and loss of 17p in combination with gain of 17q consistent with isochromosome 17q. The glioblastoma lacked all of the mutations and cytogenetic alterations seen in the medulloblastoma. Instead, the glioblastoma harbored somatic mutations in *TP53*, *STAG2*, and *GATA2*, focal high level of amplification of *PDGFRA* with a missense mutation on the amplified allele, focal high-level amplification of *MYCN*, and focal homozygous deletion of *BCOR*. These genetic findings provide support for the diagnosis of a secondary glioblastoma, rather than recurrent medulloblastoma.

A peripheral blood sample was sequenced from six of the patients allowing for assessment of potential germline variants associated with increased cancer risk. Patient #8 was found to harbor a heterozygous splice site mutation in the *MUTYH* gene, which is associated with an autosomal recessive familial gastrointestinal polyposis syndrome when biallelic germline mutations are present (either homozygous or compound heterozygous), which was not seen in this patient. No family history of colorectal adenocarcinoma or other cancers were present, and this patient's glioblastoma did not demonstrate hypermutation or a mutational signature associated with base excision repair deficiency (i.e., predominance of C>A transversions). Besides this *MUTYH* variant, no other germline alterations associated with increased cancer risk were identified in the six patients. Specifically, no truncating or known damaging missense mutations were identified involving the *TP53*, *NF1*, *CDKN2A*, *POT1*, *TSC1*, *TSC2*, *PMS2*, *MLH1*, *MSH2*, or *MSH6* genes known to be causative of familial glioma predisposition syndromes, nor were there truncating or known damaging missense mutations identified involving any genes involved in DNA double-strand break repair such as *BRCA1*, *BRCA2*, *PALB2*, *ATR*, or *ATM*.

Distinct genomic signature of radiation-associated gliomas

We next assessed the somatic mutation burden and mutational signature of the six radiation-associated gliomas in which a matched normal sample (peripheral blood) had been sequenced, allowing for accurate determination of somatic mutation status. These six tumors all demonstrated less than three somatic single nucleotide variants or small indels per Mb. The six tumors that were sequenced without a matched normal sample were all predicted to also have a low somatic mutation burden. No distinctive mutational signature was observed, such as a predominance of C>T transitions or small indels. However, the small number of somatic mutations in the approximately 2.8 Mb of the tumor genome that was sequenced precludes reliable assessment of such mutational pattern.

Chromosomal copy number analysis of the ten high-grade gliomas arising after radiation therapy revealed markedly aneuploid genomes with multiple segmental gains and losses involving several chromosomes per tumor. As ionizing radiation causes DNA double-strand breaks, we hypothesized that this marked fragmentation of the genome may have originated at the time of radiation therapy for the primary malignancy and resulted in clonal expansion of a tumor-initiating cell harboring a genomic signature that may help to differentiate radiation-induced gliomas from their spontaneous counterparts. To assess this hypothesis, we quantitated the number of intrachromosomal copy number breakpoints per genome in the 10 radiation-associated high-grade gliomas, alongside a cohort of 12 spontaneous IDH-wildtype glioblastomas in the cerebral hemispheres of adults, 12 spontaneous IDH-mutant glioblastomas in the cerebral hemispheres of adults, 12 spontaneous H3 K27M-mutant diffuse midline gliomas in children, and 12 spontaneous IDH- and H3 K27-wildtype high-grade infiltrative gliomas in children [Fig. 3 and Supplementary Tables 8 and 9 (Online
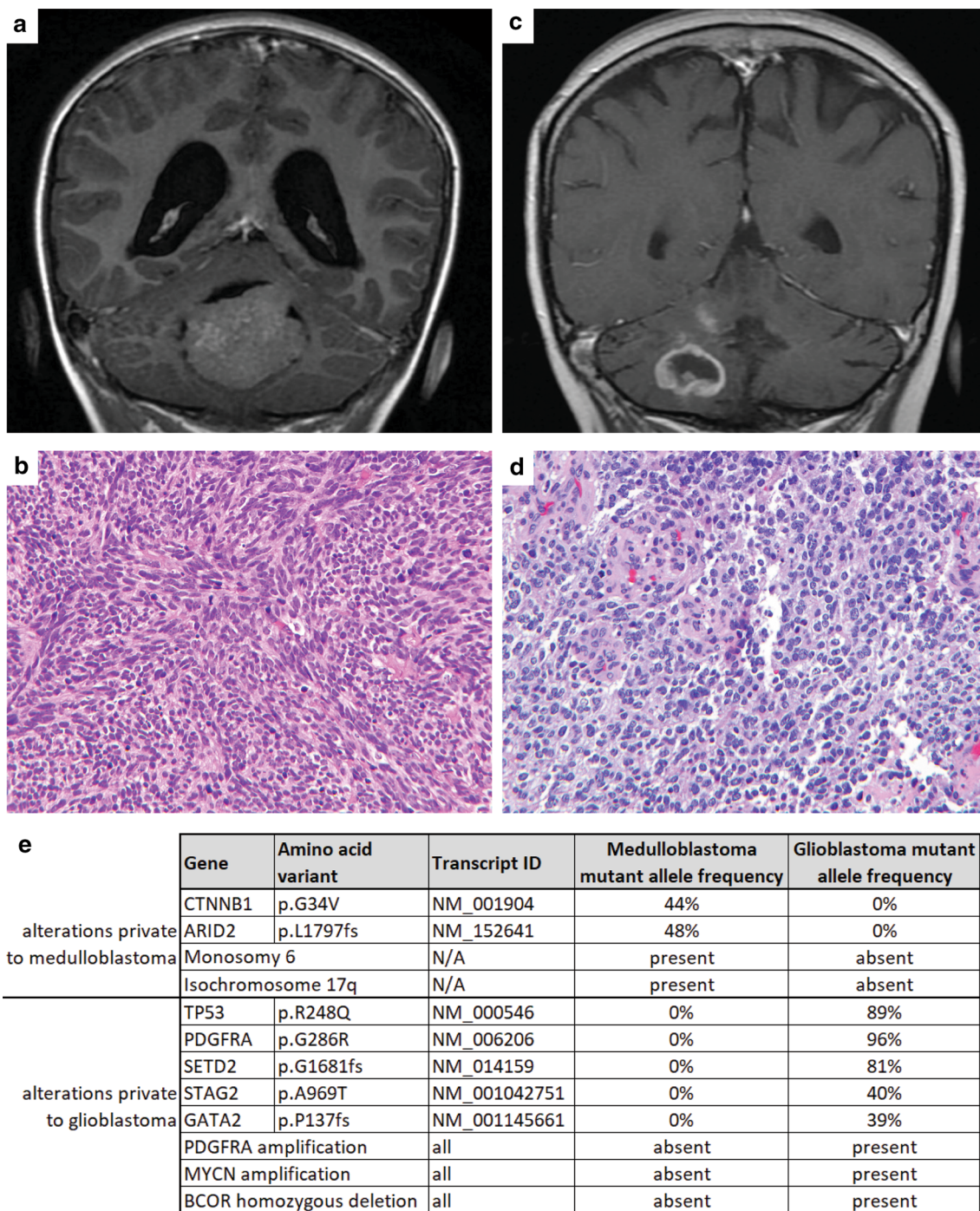
Gene	Amino acid variant	Transcript ID	Medulloblastoma mutant allele frequency	Glioblastoma mutant allele frequency
CTNNB1	p.G34V	NM_001904	44%	0%
ARID2	p.L1797fs	NM_152641	48%	0%
Monosomy 6	N/A	present	absent
Isochromosome 17q	N/A	present	absent
TP53	p.R248Q	NM_000546	0%	89%
PDGFRA	p.G286R	NM_006206	0%	96%
SETD2	p.G1681fs	NM_014159	0%	81%
STAG2	p.A969T	NM_001042751	0%	40%
GATA2	p.P137fs	NM_001145661	0%	39%
PDGFRA amplification	all	absent	present
MYCN amplification	all	absent	present
BCOR homozygous deletion	all	absent	present

alterations private to medulloblastoma (rows CTNNB1 through Isochromosome 17q)
alterations private to glioblastoma (rows TP53 through BCOR homozygous deletion)

Fig. 2 Glioblastoma arising after craniospinal radiation therapy for medulloblastoma during childhood (patient #3). **a** Coronal T1-weighted post-gadolinium magnetic resonance image at 7 years of age demonstrating medulloblastoma within the fourth ventricle. **b** Histology showing medulloblastoma of classic histologic type. **c** Coronal T1-weighted post-gadolinium magnetic resonance image at 19 years of age demonstrates a peripherally enhancing mass in the right cerebellum. **d** Histology showing a glioblastoma with microvascular proliferation. **e** Summary of the somatic alterations identified upon targeted sequencing of the medulloblastoma and radiation-associated glioblastoma

Resource 1)]. The ten radiation-associated high-grade gliomas demonstrated a median of 58 intrachromosomal copy number breakpoints per genome (range 30–128), which was significantly greater than each of the four assessed spontaneous glioma tumor entities: IDH-wildtype glioblastoma in the cerebral hemispheres of adults, median 12, range 5–34
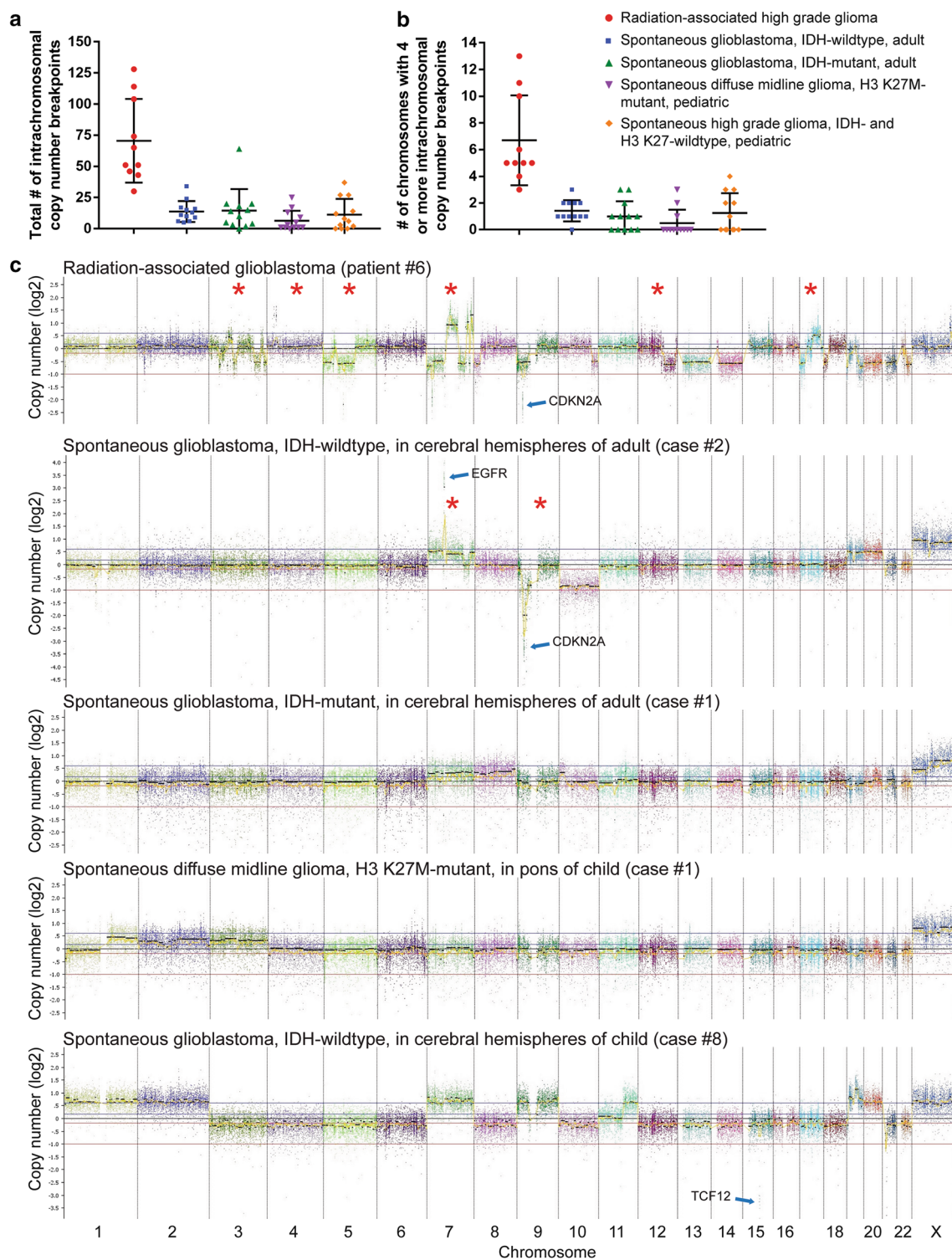
Fig. 3 High-grade gliomas arising after radiation therapy demonstrate a distinct genomic signature characterized by a large quantity of intrachromosomal copy number breakpoints. Quantitative assessment of the total number of intrachromosomal copy number breakpoints per tumor genome (**a**) and number of chromosomes with ≥4 intrachromosomal copy number breakpoints (**b**) for the 10 high-grade gliomas arising after radiation therapy, alongside 12 spontaneous IDH-wildtype glioblastomas in the cerebral hemispheres of adults, 12 spontaneous IDH-mutant glioblastomas in the cerebral hemispheres of adults, 12 spontaneous H3 K27M-mutant diffuse midline gliomas in midline structures of children, and 12 spontaneous IDH- and H3 K27-wildtype high-grade infiltrative gliomas in children. **c** Chromosomal copy number plots from representative cases of these five tumor entities. Red asterisks indicate chromosomes harboring four or more intrachromosomal copy number breakpoints

($p < 0.0001$); IDH-mutant glioblastomas in the cerebral hemispheres of adults, median 12, range 0–64 ($p < 0.0001$); H3 K27M-mutant diffuse midline gliomas in children, median 2, range 0–25 ($p < 0.0001$); IDH- and H3 K27-wildtype high-grade infiltrative gliomas in children, median 7, range 0–37 ($p < 0.0001$). We next quantitated the number of chromosomes with four or more intrachromosomal copy number breakpoints per genome in the ten radiation-associated high-grade gliomas versus the cohort of spontaneous gliomas. The ten radiation-associated high-grade gliomas demonstrated a median of five chromosomes with four or more intrachromosomal copy number breakpoints per genome (range 3–13), which was significantly greater than each of the four assessed spontaneous glioma tumor entities: IDH-wildtype glioblastoma in the cerebral hemispheres of adults, median 1, range 0–3 ($p < 0.0001$); IDH-mutant glioblastomas in the cerebral hemispheres of adults, median 1, range 0–3 ($p < 0.0001$); H3 K27M-mutant diffuse midline gliomas in children, median 0, range 0–3 ($p < 0.0001$); IDH- and H3 K27-wildtype high-grade infiltrative gliomas in children, median 1, range 0–4 ($p < 0.0001$). We next quantitated the total number of focal amplifications and focal homozygous deletions per genome in the ten radiation-associated high-grade gliomas versus the cohort of spontaneous gliomas. The ten radiation-associated high-grade gliomas demonstrated a median of four focal amplifications or homozygous deletions per genome (range 1–27), which was significantly greater than three of the four assessed spontaneous glioma tumor entities: IDH-wildtype glioblastoma in the cerebral hemispheres of adults, median 3, range 1–4 ($p = 0.09$); IDH-mutant glioblastomas in the cerebral hemispheres of adults, median 0, range 0–6 ($p = 0.0002$); H3 K27M-mutant diffuse midline gliomas in children, median 0, range 0–3 ($p < 0.0001$); IDH- and H3 K27-wildtype high-grade infiltrative gliomas in children, median 1, range 0–8 ($p = 0.004$).

The two radiation-associated low-grade gliomas histologically diagnosed as pleomorphic xanthoastrocytoma and ganglioglioma did not demonstrate an increased number of intrachromosomal copy number breakpoints or focal amplifications and homozygous deletions. The pleomorphic xanthoastrocytoma (case #11) demonstrated loss of chromosomes 1p, 9, and 10q. The ganglioglioma (case #12) demonstrated seven intrachromosomal copy number breakpoints that included focal homozygous deletion of the *SMARCB1* tumor suppressor on chromosome 22q.

Discussion

Here, we studied the genetic features of 12 gliomas arising after radiation therapy that fulfilled the criteria for a radiation-induced secondary malignancy as proposed by Cahan et al., which include tumor formation within the prior radiation field, absence of familial tumor predisposition syndrome, and different pathologic tumor types between the primary and secondary neoplasms [6]. As previously described, the majority of the radiation-associated gliomas in our cohort (10/12) were high-grade infiltrative astrocytomas, either anaplastic astrocytoma or glioblastoma. In cases with available clinical follow-up, all patients with high-grade gliomas had poor outcomes.

We find that secondary gliomas arising after radiation therapy lack alterations in *IDH1*, *IDH2*, *H3F3A*, *HIST1H3B*, *HIST1H3C*, *TERT* (including promoter region), and *PTEN*, which genetically define the major subtypes of diffuse gliomas in children and adults. Thus, radiation-induced gliomas appear to be molecularly distinct from the IDH-mutant diffuse lower-grade gliomas arising in the cerebral hemispheres of adults. Additionally, radiation-induced gliomas appear to be molecularly distinct from H3 K27M-mutant diffuse midline gliomas and from H3 G34R/V-mutant diffuse gliomas in the cerebral hemispheres of children and young adults. In contrast to IDH-wildtype glioblastomas arising in the cerebral hemispheres in adults, radiation-induced gliomas lack the combination of trisomy seven and monosomy ten that cytogenetically characterize the vast majority of spontaneous IDH-wildtype glioblastomas in adults. Additionally, they lack the *TERT* promoter hotspot mutations and *PTEN* mutation/deletion that genetically characterize the vast majority of spontaneous IDH-wildtype glioblastomas in adults.

We find that radiation-associated high-grade gliomas, which comprised 10 of the 12 cases in our cohort, are genetically characterized by a high frequency of biallelic *TP53* inactivation, *CDK4* amplification or *CDKN2A* homozygous deletion, and amplifications or rearrangements involving receptor tyrosine kinase and Ras–Raf–MAP kinase pathway genes including *PDGFRA*, *MET*, *BRAF*, and *RRAS2*. We speculate that *TP53* mutation is selected for early in the development of radiation-induced gliomas to permit survival and expansion of the tumor-initiating cell with numerous chromosomal rearrangements induced by the ionizing radiation. Notably, *TP53* mutations have also been identified at high frequency in radiation-induced sarcomas [4]. Similar to spontaneous high-grade gliomas in both children and adults, radiation-associated high-grade gliomas have frequent disruption of the cell cycle regulatory genes such as *CDK4* and *CDKN2A*. Additionally, they share frequent activation of receptor tyrosine kinase genes and Ras–Raf–MAP kinase pathway genes. However, in contrast to IDH-wildtype glioblastomas in the cerebral hemispheres of adults [8, 9], radiation-associated high-grade gliomas only rarely harbor *EGFR* amplification or mutation and instead more frequently demonstrate *PDGFRA* or *MET* amplifications or mutations. Compared with both high-grade gliomas in children and IDH-wildtype glioblastomas in adults [8, 9, 19, 32], radiation-associated high-grade gliomas only rarely harbor

NF1 inactivation and instead more frequently demonstrate *BRAF* rearrangement or *RRAS2* focal high-level amplifications, the latter of which is not known to be recurrently present in any spontaneous glioma subtype. These findings highlight potential vulnerabilities to targeted therapeutics, particularly kinase inhibitors targeting activated PDGFRA, MET, or MEK.

We identified a distinct genomic signature of secondary high-grade gliomas arising after radiation therapy compared to their spontaneous counterparts. This included a significantly increased quantity of intrachromosomal copy number breakpoints per genome, number of chromosomes harboring multiple intrachromosomal copy number breakpoints, and focal amplifications/homozygous deletions. This large quantity of intrachromosomal copy number breakpoints was distributed across several chromosomes in the genome, and was not limited to one or two chromosomes that had undergone chromothripsis, which is sometimes seen for chromosomes 7 and 9 in spontaneous IDH-wildtype glioblastomas as the likely mechanism for causing *EGFR* amplification and *CDKN2A* homozygous deletion. Thus, in addition to an increased quantity of the total number of intrachromosomal copy number breakpoints per genome, the presence of several chromosomes harboring an increased number of intrachromosomal copy number breakpoints provides additional specificity for distinguishing radiation-associated gliomas from their spontaneous counterparts. Furthermore, we find a low burden of somatic single nucleotide variants in radiation-associated gliomas, which is similar to the vast majority of spontaneous gliomas. These findings provide insight into the underlying mechanism by which ionizing radiation leads to secondary malignancies. It suggests that ionizing radiation causes DNA double-strand breaks in a tumor-initiating cell at the time of therapy for the primary malignancy, which after a variable period of dormancy undergoes clonal expansion, likely following acquisition of the additional genetic alterations required for gliomagenesis. These radiation-induced double-strand breaks lead to a distinct genomic signature that differentiates these tumors from their spontaneous counterparts and is likely responsible for promoting the amplifications of oncogenes (e.g., *PDGFRA*, *MET*, *RRAS2*), homozygous deletions of tumor suppressor genes (e.g., *CDKN2A*), and rearrangements of oncogenes (e.g., *BRAF*) that characterize radiation-induced gliomas. This hypothesis is supported by a mouse model of radiation-induced gliomagenesis whereby gamma irradiation of Cdkn2a null mice resulted in glioblastomas with frequent Met amplification [7].

Two of the secondary gliomas in this cohort were histologically low-grade glial neoplasms resembling pleomorphic xanthoastrocytoma and ganglioglioma. Interestingly, the pleomorphic xanthoastrocytoma harbored the combination of monosomy 1p and *KIAA1549–BRAF* fusion that defines diffuse leptomeningeal glioneuronal tumor and lacked the presence of *CDKN2A* homozygous deletion that is present in the vast majority of pleomorphic xanthoastrocytomas [25–27]. The ganglioglioma harbored *SMARCB1* focal homozygous deletion that is not a known recurrent alteration in ganglioglioma and also lacked an identifiable alteration in the Ras–Raf–MAP kinase pathway, which is present in the vast majority of gangliogliomas [23]. Thus, low-grade glial and glioneuronal tumors arising after radiation therapy may be distinct from their spontaneous counterparts and challenging to diagnostically classify even with supplemental molecular characterization. Notably, both of these low-grade gliomas lacked an increase in the quantity of intrachromosomal copy number breakpoints and focal amplifications/homozygous deletions observed in the radiation-associated high-grade gliomas. Whether or not these two tumors were actually radiation induced is therefore uncertain. However, the pathogenic alterations identified in both tumors (*KIAA1549–BRAF* fusion and *SMARCB1* homozygous deletion) were caused by chromosomal breaks rather than single nucleotide variants, which may have been induced by ionizing radiation at the time of therapy for the primary malignancy.

Overall, we identify the genetic landscape of secondary gliomas arising after radiation therapy for childhood malignancies and demonstrate a distinct genomic signature that differentiates these tumors from their spontaneous counterparts. These findings have significant diagnostic and therapeutic implications for long-term survivors of childhood cancers.

Compliance with ethical standards

Ethical approval This study was approved by the Committee on Human Research of the University of California, San Francisco, with a waiver of patient consent.

Conflict of interest The authors declare that they have no competing interests related to this study.

References

1. Agnihotri S, Suppiah S, Tonge PD et al (2017) Therapeutic radiation for childhood cancer drives structural aberrations of NF2 in meningiomas. Nat Commun 8:186

2. Alexandrov LB, Nik-Zainal S, Wedge DC et al (2013) Signatures of mutational processes in human cancer. Nature 500:415–421

3. Behjati S, Gundem G, Wedge DC et al (2016) Mutational signatures of ionizing radiation in second malignancies. Nat Commun 7:12605

4. Brachman D, Hallahan D, Beckett M, Yandell D, Weichselbaum R (1991) p53 gene mutations and abnormal retinoblastoma protein in radiation-induced human sarcomas. Cancer Res 51:6393–6396

5. Brat DJ, James CD, Jedlicka AE et al (1999) Molecular genetic alterations in radiation-induced astrocytomas. Am J Pathol 154:1431–1438

6. Cahan W, Woodard H, Higinbotham N, Stewart F, Coley B (1948) Sarcoma arising in irradiated bone: report of eleven cases. Cancer 82:8–34

7. Camacho CV, Todorova PK, Hardebeck MC et al (2015) DNA double-strand breaks cooperate with loss of Ink4 and Arf tumor suppressors to generate glioblastomas with frequent Met amplification. Oncogene 34:1064–1072

8. Cancer Genome Atlas Research Network (2008) Comprehensive genomic characterization defines human glioblastoma genes and core pathways. Nature 455:1061–1068

9. Cancer Genome Atlas Research Network (2013) The somatic genomic landscape of glioblastoma. Cell 155:462–477

10. Cancer Genome Atlas Research Network (2015) Comprehensive, integrative genomic analysis of diffuse lower-grade gliomas. N Engl J Med 372:2481–2498

11. Chowdhary A, Spence AM, Sales L, Rostomily RC, Rockhill JK, Silbergeld DL (2012) Radiation associated tumors following therapeutic cranial radiation. Surg Neurol Int 3:48

12. Donson AM, Erwin NS, Kleinschmidt-DeMasters BK, Madden JR, Addo-Yobo SO, Foreman NK (2007) Unique molecular characteristics of radiation-induced glioblastoma. J Neuropathol Exp Neurol 66:740–749

13. Eckel-Passow JE, Lachance DH, Molinaro AM et al (2015) Glioma groups based on 1p/19q, IDH, and TERT promoter mutations in tumors. N Engl J Med 372:2499–2508

14. Fontebasso AM, Schwartzentruber J, Khuong-Quang DA et al (2013) Mutations in SETD2 and genes affecting histone H3K36 methylation target hemispheric high-grade gliomas. Acta Neuropathol 125:659–669

15. Foray N (2016) Victor Despeignes, the forgotten pioneer of radiation oncology. Int J Radiat Oncol Biol Phys 96:717–721

16. Henson JW, Hobbs W, Chakravarti A, Louis DN (2005) Alterations in p53, p21, and MIB-1 labeling index in primary human astrocytomas following radiation therapy. J Neurooncol 74:151–154

17. Iorgulescu JB, Van Ziffle J, Stevers M et al (2018) Deep sequencing of WNT-activated medulloblastomas reveals secondary SHH pathway activation. Acta Neuropathol 135:635–638

18. Kline CN, Joseph NM, Grenert JP et al (2017) Targeted next-generation sequencing of pediatric neuro-oncology patients improves diagnosis, identifies pathogenic germline mutations, and directs targeted therapy. Neuro-Oncol 19:699–709

19. Mackay A, Burford A, Carvalho D et al (2017) Integrated molecular meta-analysis of 1000 pediatric high-grade and diffuse intrinsic pontine glioma. Cancer Cell 32:520–537

20. Nakao T, Sasagawa Y, Nobusawa S et al (2017) Radiation-induced gliomas: a report of four cases and analysis of molecular biomarkers. Brain Tumor Pathol 34:149–154

21. Paugh BS, Qu C, Jones C et al (2010) Integrated molecular genetic profiling of pediatric high-grade gliomas reveals key differences with the adult disease. J Clin Oncol 28:3061–3068

22. Pekmezci M, Stevers M, Phillips JJ et al (2018) Multinodular and vacuolating neuronal tumor of the cerebrum is a clonal neoplasm defined by genetic alterations that activate the MAP kinase signaling pathway. Acta Neuropathol 135:485–488

23. Pekmezci M, Villanueva-Meyer JE, Goode B et al (2018) The genetic landscape of ganglioglioma. Acta Neuropathol Commun 6:47

24. Phi JH, Park AK, Lee S et al (2018) Genomic analysis reveals secondary glioblastoma after radiotherapy in a subset of recurrent medulloblastomas. Acta Neuropathol 135:939–953

25. Phillips JJ, Gong H, Chen K et al (2016) Activating NRF1-BRAF and ATG7-RAF1 fusions in anaplastic pleomorphic xanthoastrocytoma without BRAF p. V600E mutation. Acta Neuropathol 132:757–760

26. Phillips JJ, Gong H, Chen K, Joseph NM, van Ziffle J, Bastian BC, Grenert JP, Kline CN, Mueller S, Banerjee A, Nicolaides T, Gupta N, Berger MS, Lee HS, Pekmezci M, Tihan T, Bollen AW, Perry A, Shieh JTC, Solomon DA (2018) The genetic landscape of anaplastic pleomorphic xanthoastrocytoma. Brain Pathol. https://doi.org/10.1111/bpa.12639

27. Rodriguez FJ, Schniederjan MJ, Nicolaides T, Tihan T, Burger PC, Perry A et al (2015) High rate of concurrent BRAF-KIAA1549 gene fusion and 1p deletion in disseminated oligodendroglioma-like leptomeningeal neoplasms (DOLN). Acta Neuropathol 129:609–610

28. Sahm F, Toprak UH, Hübschmann D et al (2017) Meningiomas induced by low-dose radiation carry structural variants of NF2 and a distinct mutational signature. Acta Neuropathol 134:155–158

29. Salvati M, D'Elia A, Melone GA et al (2008) Radio-induced gliomas: 20-year experience and critical review of the pathology. J Neurooncol 89:169–177

30. Solomon DA, Wood MD, Tihan T et al (2016) Diffuse midline gliomas with histone H3-K27M mutation: a series of 47 cases assessing the spectrum of morphologic variation and associated genetic alterations. Brain Pathol 26:569–580

31. Walter AW, Hancock ML, Pui CH et al (1998) Secondary brain tumors in children treated for acute lymphoblastic leukemia at St Jude Children's Research Hospital. J Clin Oncol 16:3761–3767

32. Wu G, Diaz AK, Paugh BS et al (2014) The genomic landscape of diffuse intrinsic pontine glioma and pediatric non-brainstem high-grade glioma. Nat Genet 46:444–450

33. Yamanaka R, Hayano A, Kanayama T (2018) Radiation-induced gliomas: a comprehensive review and meta-analysis. Neurosurg Rev 41:719–731

Affiliations

Giselle Y. López[1,2] · Jessica Van Ziffle[1,3] · Courtney Onodera[1,3] · James P. Grenert[1,3] · Iwei Yeh[1,3,4] · Boris C. Bastian[1,3,4] · Jennifer Clarke[5,6] · Nancy Ann Oberheim Bush[5,6] · Jennie Taylor[5,6] · Susan Chang[5] · Nicholas Butowski[5] · Anuradha Banerjee[7] · Sabine Mueller[6,7] · Cassie Kline[6,7] · Joseph Torkildson[8] · David Samuel[9] · Aleli Siongco[10] · Corey Raffel[2] · Nalin Gupta[2,11] · Sandeep Kunwar[2] · Praveen Mummaneni[2] · Manish Aghi[2] · Philip Theodosopoulos[2] · Mitchel Berger[2] · Joanna J. Phillips[1,2] · Melike Pekmezci[1] · Tarik Tihan[1] · Andrew W. Bollen[1] · Arie Perry[1,2] · David A. Solomon[1,3]

1 Department of Pathology, University of California, San Francisco, CA, USA

2 Department of Neurological Surgery, University of California, San Francisco, CA, USA

3 Clinical Cancer Genomics Laboratory, University of California, San Francisco, CA, USA

4 Department of Dermatology, University of California, San Francisco, CA, USA

5 Division of Neuro-Oncology, Department of Neurological Surgery, University of California, San Francisco, CA, USA

6 Department of Neurology, University of California, San Francisco, CA, USA

7 Division of Hematology/Oncology, Department of Pediatrics, University of California, San Francisco, CA, USA

8 Department of Hematology/Oncology, UCSF Benioff Children's Hospital Oakland, Oakland, CA, USA

9 Department of Hematology/Oncology, Valley Children's Hospital, Madera, CA, USA

10 Department of Pathology, Valley Children's Hospital, Madera, CA, USA

11 Department of Pediatrics, University of California, San Francisco, CA, USA